Supplementary Materials to
"Hydrogel microrobots actuated by optically generated vapour bubbles"

Bubble generation and temperature rise in microrobot system

A laser pulse is used to generate the bubbles that drive the hydrogel microrobots. The laser energy is absorbed by the substrate, heating the liquid and creating a microbubble. The bubble collapses once the laser pulse is over. A typical experiment uses 160-µs pulses at a repetition rate of 20 Hz.

Cells under manipulation should be kept below their maximum physiological temperature (usually 37 °C), so the temperature in the microrobot system was tested to verify biocompatibility. The thermoresponsive polymer poly(N-isopropylacrylamide), or PNIPAAm was used to detect the temperature of the liquid surrounding the hydrogel microrobots. PNIPAAm is soluble in water at room temperature, but forms a gel when the temperature exceeds 32 °C [ref. 1]. Thus, the presence of gelled PNIPAAm means that the temperature of the solution is greater than 32 °C. For a laser pulse width of 160 µs and a pulse frequency of 20 Hz, PNIPAAm gelation was observed in an area with a diameter of 14.5 µm when ambient temperature was 20˚C. This corresponds to the highest amount of optical energy of all the laser pulses used here for cellular manipulation. The diameter of the PNIPAAm gel is much smaller than the minimum diameter (80 µm) of the current microrobot. More heat may be retained when a microrobot is actually present around a laser-induced bubble, due to more limited heat dissipation. However, when the experiment was repeated with a hydrogel microrobot present, no gelation was observed outside the region covered by the hydrogel microrobot structure. These PNIPAAm experiments indicate that the microrobot keeps cells at a safe temperature by maintain adequate distance from the heated area on the substrate. Furthermore, the microrobot diameter is also significantly larger than the diameter of the laser spot, ensuring that the cells are not irradiated with high-intensity light.
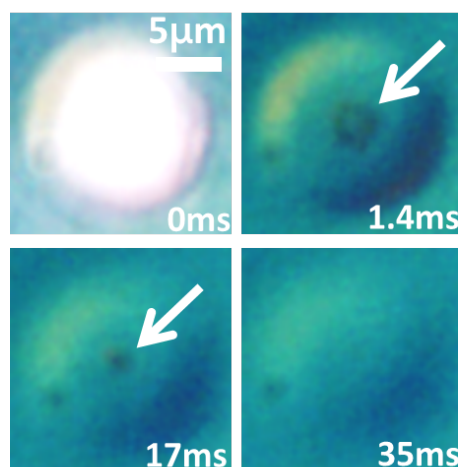

Fig. S1 Generation and collapse of a bubble in the 10% PNIPAAm solution in deionized water. The laser pulse width is 160 µs at a frequency of 20 Hz. The circular area visible in the last three frames is due to the gelation of PNIPAAm. The bubble marked by the white arrows has a diameter of 3.4 µm immediately after the laser pulse, and it dissolves into the solution within 35 ms. Due to refraction at the surface of the layer of water, the laser spot appears larger than its actual size.

Hydrogel microrobot fabrication

To form the hydrogel microrobots, 1% of Irgacure 819 (Ciba Specialty Chemicals) was used as photoinitiator for the polymerization of PEGDA. The pre-polymer was pipetted into a fluidic chamber with a height of 50 µm, and then exposed to UV light to initiate the polymerization. A

modified commercial projector (Dell 2400MP) was used as the light source. The UV filter of the projector was removed to provide an increased output of the light wavelengths absorbed by the photoinitiator. The desired microrobot shape was drawn in Microsoft PowerPoint software and displayed on the projector, selectively creating PEGDA hydrogels. This fabrication method allows the microrobot shape to be easily altered by adjusting the microrobot pattern in software. The resulting hydrogel structures are rinsed with isopropanol, and transferred into the fluid reservoir using a 33-gauge needle. The PowerPoint pattern used to create the hydrogel structure had a dark spot in the centre of the disk (Fig. 2). Light refraction in the projection system led to the formation of the concave cavities in the centre of the disk.
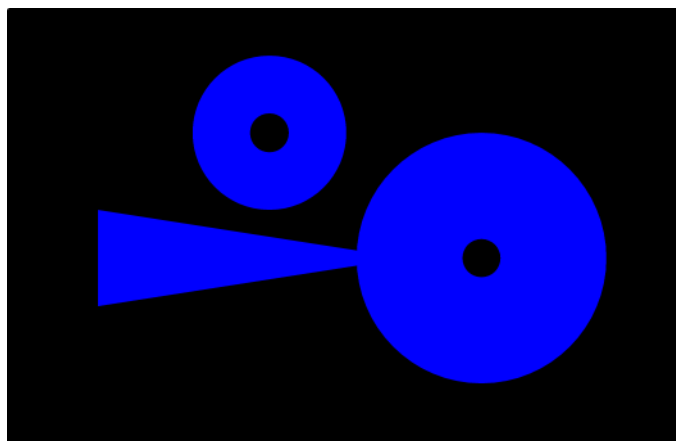

Fig. S2 The optical patterns used for the photopolymerization of the hydrogel microrobots.

Microrobot actuation mechanism

The toroidal profile of the thermocapillary flow can be observed by using 0.7-μm-diameter beads as tracer particles (Bangs Laboratories, Inc., Styrene/Vinyl-COOH/41% Magnetite). The axially symmetric parallel component can be observed from the bead trajectories (Fig. 3). The trajectory of a single bead in toroidal circulation is also demonstrated in the video S-1.

In an optothermal system such as the one used here, two other effects may cause fluidic flows: the thermocapillary flow at the liquid surface at the top of the fluid reservoir[2] and natural convection. The heating of the substrate can possibly create a temperature gradient at the top surface of the liquid layer, which could give rise to another thermocapillary flow in addition to the one surrounding the bubble. Natural convection is due to a change in the liquid density distribution as the liquid is heated unevenly. Hotter, less dense portions of a liquid move upward, and colder, denser portions of the liquid move downward due to gravity. However, these two fluid flows are not significant, and the induced thermocapillary flow around the laser-driven bubble is the dominant actuation force in this microrobotic system. This was verified by quantifying the velocity of the 0.7-μm-diameter beads in Fig. 3. The rate at which the 0.7-μm beads were attracted towards the centre of the laser-generated bubble was measured in three different configurations of the fluid reservoir: 1) an open, uncovered fluid reservoir, as shown in Fig. 1a of the main paper; 2) an enclosed fluid reservoir; and 3) an enclosed fluid reservoir, inverted from the orientation shown in Fig. 1a of the main paper, so that the α-Si coated surface is on the top of the fluid chamber, and with the laser projected from above. The first configuration reflects fluid flow under normal microrobot operating conditions. The second configuration eliminates the air/water interface at the top of the fluid reservoir, and thus the corresponding thermocapillary flow at this surface is negligible. The third configuration also eliminates the thermocapillary flow at the liquid surface, but it can additionally be used to determine the

contribution of the natural convection. In this configuration, the natural convective flow will be reversed as compared to the first configuration. The measured fluid flow velocities for the three different configurations have no significant difference (Fig. 4). Thus, the primary source of the fluid flow is the thermocapillary effect from the temperature gradient surrounding the laser-induced bubble.
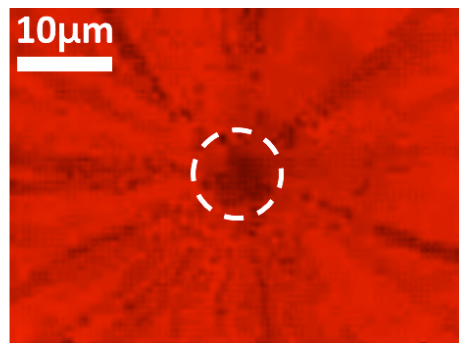

Fig. S3 The toroidal thermocapillary flow traced by 0.7-μm-diameter beads. This image is a composite of a series of 7,000 images recorded over 10 seconds. The laser spot is marked by the dashed circle.
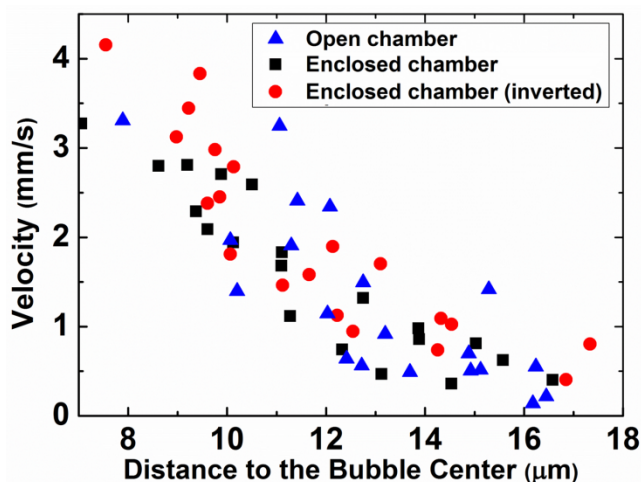

Fig. S4 Measured velocity of 0.7-μm-diameter beads in the fluid flow surrounding the bubble for three different configurations of the fluid reservoir. The velocity represents movement towards the bubble. The laser had a pulse width of 30 μs at a frequency of 60 Hz.

Factors affecting microrobot actuation

Increasing the laser pulse frequency or the laser pulse width can drive the microrobot faster. This is shown in Fig. 4 of the main paper. Fig. 5 also shows an extended data set for the measurements shown in Fig. 4 in the main paper.

However, increasing pulse frequency or pulse width also causes the microrobot to be levitated higher from the substrate due to a larger vapour bubble and stronger fluidic flow surrounding the bubble. This may leave the microrobot unable to manipulate objects smaller than the height of the levitation, as those objects will slip underneath the hydrogel structure of the microrobot. For example, consider the 140-μm-diameter microrobots actuated with a 20-Hz laser pulse frequency. A pulse width of 380 μs is sufficient to levitate the microrobot more than 20 μm above the substrate, rendering it unable to interact with a 20-μm-diameter polystyrene bead. Under this actuation condition, the microrobot moves over the beads instead of pushing the beads

with the edge of the structure. Pulse widths larger than 380 µs at 20 Hz results in a bubble that continues growing in size, finally levitating the microrobot high enough to be in a metastable state; if the laser is scanned along the substrate, perturbations in the thermocapillary flow can cause the hydrogel microrobot to flip. Increasing the pulse frequency has a similar effect. Smaller microrobots are more susceptible to these issues, as they have less mass and are more easily elevated above the substrate. Thus, the microrobot levitation presents a limitation on the maximum manipulation velocity that can be used. The laser pulse frequency and pulse width need to be optimized based on the microrobot size and the size of the objects being manipulated.
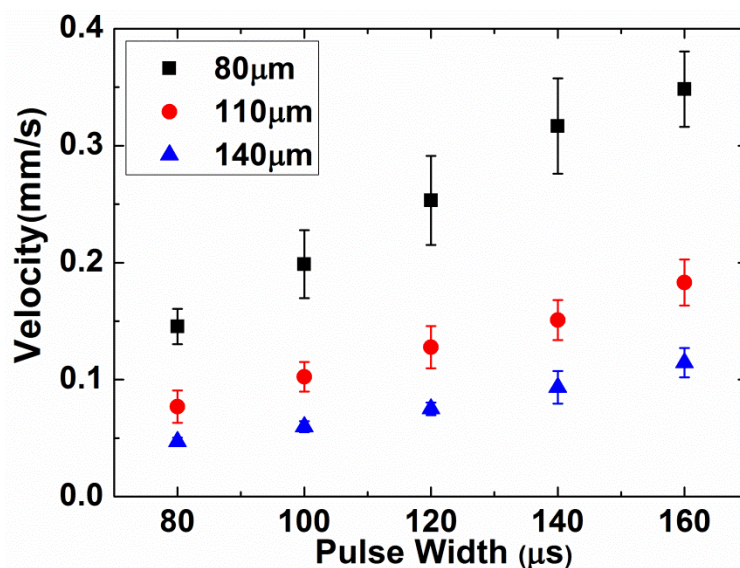

Fig. S5 The effect of longer laser pulse widths for a laser pulse frequency of 20 Hz. The different data sets represent hydrogel microrobots with different diameters.

Description of the supplementary videos

S-1 Bead circulation:
The trajectory of a single 0.7-µm-diameter bead in toroidal circulation is shown in the video S-1. The laser frequency is 60 Hz and the laser pulse width is 30 µs.

S-2 Cooperative assembly:
Two 20-µm-diameter polystyrene beads were moved in parallel by two independently operated hydrogel microrobots to either side of a bead located in the centre of the field of view.

References
1 K. Kubota, S. Fujishige and I. Ando, *Polymer Journal*, 1990, **22**, 15-20.
2 W. Hu and A. T. Ohta, *Microfluidics and Nanofluidics*, 2011, **11**, 307-316.